Engineering Research Journal
journal homepage: https://erj.journals.ekb.eg/

Seismic Performance of Tall Buildings having Steel Plate Shear Wall Combined with BRB-Outriggers

Nehal M. Ayash[1, *], Fattouh M. F. Shaker[2], Fatma Abdelmohsen Mahmoud[3]

[1] Associate Professor, Civil Engineering Department, Faculty of Engineering, Mataria, Helwan University
[2] Professor of Steel Structures and bridges, Civil Engineering Department, Faculty of Engineering, Mataria, Helwan University
[3]M. Sc. Student, Civil Engineering Department, Faculty of Engineering, Mataria, Helwan University
*Corresponding Author E-mail: nehal82ayash@m-eng.helwan.edu.eg

Abstract. Several structures have employed steel plate shear walls (SPSWs). It might cause excessive lateral drift and substantial seismic demands on vertical boundary elements (VBEs). A sensible workaround for SPSW systems is to install an outrigger as a dissipated system in place of the adjacent bay of the SPSWs. This will disperse some of the overturning forces to the adjacent columns, thereby reducing lateral drifts and seismic demand on the VBEs. Nonlinear time history studies are performed for 12- and 20-story free-standing SPSWs with different wall bay width-to-depth ratios and SPSWs combined with Buckling restrained brace outrigger (BRB-O). The effectiveness of the BRB-O on the overall seismic behavior is investigated. These elements are placed in single and double BRB-Os at various locations along the wall. The findings indicated that adding BRB-O significantly reduces lateral responses. Positioning a single BRB-O in the stories near the middle height of the SPSW or above (especially at ¾ of the structure's height from the base) will improve its stiffness more than that placed in the below stories. The most effective way to position the double BRB-Os is to place one at the top and the other at a high level of the structure's height, particularly if the other outrigger is positioned at ¾ of the structure's height. It is more effective to add double BRB-Os where one is located at the top story rather than between inter-stories. The width-to-depth ratio of the web panel and outrigger width influences the decrease in the VBE's axial forces.

Keywords: Nonlinear Time History Analysis; Steel Plate Shear Wall (SPSW); Buckling R strained Brace (BRB); Outrigger; Drift; Plastic Hinges.

1 Introduction

A standard un-stiffened steel plate shear wall (SPSW) is made up of thin steel plates surrounded by steel beams as horizontal boundary elements (HBEs) and steel columns as vertical boundary elements (VBEs). These beams and columns can be one or more bays wide and several stories high, and they can

DOI: 10.21608/erj.2024.310750.1086
Received 08 August 2024; Received in revised form 19 September 2024; Accepted 20 September 2024
Available online 01 December 2024

have simple beam-to-column connections that resist shear or other moments. In a standard un-stiffened SPSW system, infill plates are often quite thin and give way at very low shear loads. The primary method for mitigating the shear resulting from lateral loadings is the inclined post-buckling tension field that develops in the infill plate (Fig. 1) [1].

Steel plate shear walls provide a few key advantages over reinforced concrete (RC) shear walls. These include a much thinner steel infill plate, a smaller structural weight, and a smaller footprint. More usable floor area is available due to the notable reduction in wall thickness and footprint, particularly in tall structures with extremely thick RC shear walls. Additionally, the SPSW structure and foundation are subject to less seismic stress because of the decreased structural weight. Reduced susceptibility to localized fractures is the primary benefit of the steel plate shear wall over the concentric braced structure.

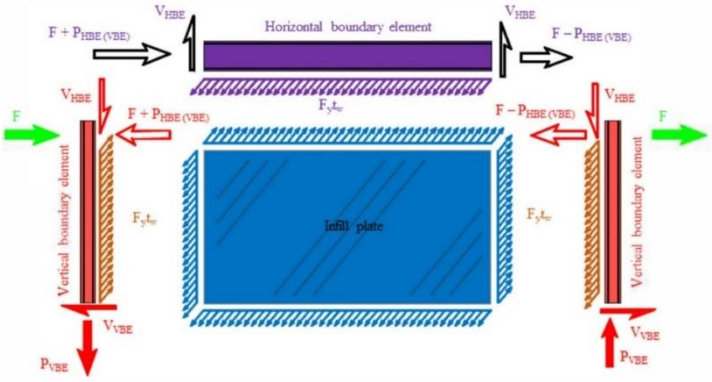

Fig. 1. Load distribution of the standard SPSW [1]

Thorburn and Montgomery (1983) [2] suggested a strip modeling that took into account the post-buckling strength in the infill plate. The strength and stiffness of the boundary HBE and VBE components, which anchor the pull-in forces generated by tension field action, determine the SPSW panel's ultimate strength. The hysteresis behavior exhibited by the infill plate closely resembles that of a slender braced system, notably characterized by significant pinching behavior within its loops. This observed pinching phenomenon of infill plates manifested during cyclic tests conducted on SPSW specimens featuring simply connected boundary frames [3], [4]. In SPSW systems, the AISC Seismic Provisions [5] incorporate a boundary frame with rigid connections and sections that are seismically compact. As shown in Fig. 2, the boundary frame greatly enhances the energy dissipation capacity and the hysteresis response. The infill plate has a similar hysteresis to the slender braced system, and the hysteresis loops show substantial pinching behavior [6]. The pinching characteristics of infill plates were shown in cyclic tests on SPSW specimens with simply connected boundary frames [7].

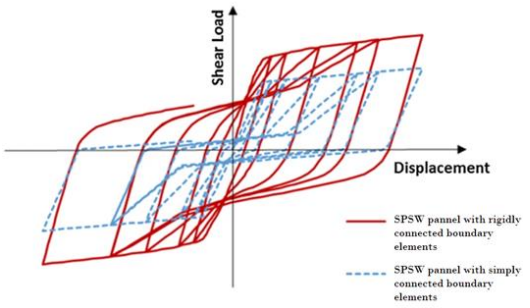

Fig. 2. Hysteresis characteristic of the SPSW system with different boundary frame connections [6]

For structures in regions with moderate to high seismicity, steel plate shear walls (SPSW) designed following AISC seismic standards offer a reliable lateral load-resisting system. The intended performance in terms of seismic behavior, including input energy, story drift, base shear, and roof center of mass displacement, has been shown by structures with steel shear walls at varying heights. Compared to 3- and 6-story constructions, the 12-story structure produced substantially superior outcomes [7]. The energy absorption of the steel shear wall is dependent on the stiffness of the surrounding component [8&9].

In tall structures, this technique does have certain drawbacks. One major drawback is that the total structural system has relatively low lateral stiffness, which could lead to significant inter-story drifts. Although plastic hinges are permitted at both ends of HBEs and the base of VBEs, HBEs, and VBEs are proposed to design with remaining elastic under the forces generated by totally yielding plates. This design philosophy is well-known as the capacity design method, which uses the un-stiffened slender plates and takes the post-buckling strength of the infill plate into consideration when calculating the capacity of SPSW. Procedures for the capacity design of the vertical and horizontal boundary elements have been proposed by [10], [11], and [13] to guarantee a ductile failure mode arising from infill plate yielding under cyclic loading. The AISC Seismic Provisions for Structural Steel Buildings [5] stipulate boundary frame members must follow those capacity design procedures. This approach leads to high design forces in the VBEs, necessitating the use of large column sections as well as increased foundation demands. Bulky VBE portions reduce the building's rentable space, increase the structure’s weight, and are uneconomic. The very strong axial forces in the vertical boundary elements constitute another major drawback. Furthermore, in the design of unstiffened SPSWs, the column overturning moment is countered by axial coupling loads, while the infill plate's diagonal tension field effectively resists the shear force in the story. To comply with welding and handling requirements, the infill plate thickness is often made thicker than what is structurally necessary.

Outriggers are utilized in most high-rise structures worldwide as a means of mitigating these forces. A system that effectively addresses the ensuing shear and bending displacements may be formed by combining an outrigger with a steel shear wall. Gholipour et al. (2014) [14] and Meisam et al. (2017) [13] have proposed an alternative solution that involves adding outriggers to the SPSW system like the approaches suggested by Akbar and Khoshkalam (2020) [6], as beams in all stories and web plate panels in different positions, respectively. This approach can significantly reduce the lateral displacements and seismic loads on the Vertical Boundary Elements (VBEs) by redistributing a portion of the overturning forces to the adjacent columns. Instead of adding an outrigger as slender panels that have low initial stiffness or beams at all stories, which may have a notable weight to the system even after the reduction in the main system elements, we can use an outrigger truss.

Buckling Restrained Braces (BRBs) have been integrated into buildings in the US, Canada, China, Turkey, and New Zealand and gained popularity in the construction sector [15], such as buckling-restrained braced frames and retrofit civil structures. Extensive research has been conducted on the performance of BRB braces [17], [18]. In high-rise buildings, strengthened stories are floors with outriggers connecting the core wall with the perimeter columns. "High-rise structural system with the energy-dissipating story" is a structural system that utilizes energy-dissipating technology proposed by [13].

According to the literature review, using outrigger systems can reduce the needed higher stiffness of VBEs (bigger dimensions) to overcome the relatively low lateral stiffness of SPSW. Because of the global buckling of bracing and the local buckling of chords following flexural yielding, the conventional outrigger systems showed a quick fall after attaining their peak strength and a poor ability for dissipating

energy. Better energy absorption than traditional outrigger systems is one of the advantages of using Buckling Restrained Braces (BRBs) as outrigger systems. To improve the seismic performance of a free-standing, unstiffened steel plate shear wall, this paper presents a novel approach of SPSW with outriggers that uses buckling restrained braces (BRBs), which replace the ordinary bracing outrigger.

2 Objective

This study investigates the seismic responses of mid- and high-rise buildings with unstiffened SPSW structural systems as lateral load-resisting systems, both with and without Buckling Restrained Brace (BRB) trusses acting as outriggers. The goal is to determine how well the outriggers contribute to the structural system's improved seismic performance. This research offers valuable insights into various factors that influence the behavior and efficiency of these dual systems and contributes to the development of the presented BRB outrigger efficiency. Parameters under investigation included mid- and high-rise SPSWs and the wall bay width-to-depth ratio (L/H). Furthermore, the optimal placement of single and double BRB-O systems in structures experiencing inelastic behavior is the main goal of this research.

3 Finite Element Modeling and Verification

3.1 Verification Model Details

This verification is carried out using a model developed by Meisam et.al. (2017) [13]. With the same floor masses, dead and live loads as the modified 9-story SAC model buildings [19], the case study of the 12- and 20-story free-standing SPSW systems under consideration was created. Fig. 3 displays the plan layouts of both SPSW systems.

Steel plate thickness, horizontal boundary elements (HBEs), vertical boundary elements (VBEs), outer columns (OCs), and outer beams (OBs) for a 12-story structure are determined to be 3.1 mm, W14x53, W36x395, W12x65, and W14x22, respectively [13]. For a 20-story building, the steel plate thickness, HBEs, VBEs, OCs, and OBs are considered as 0.91 mm, W24x68, W36x194, W8x35, and W14x22, respectively [13]. The 3.96 m story height was considered for two systems. The narrow SPSWs (3.6 meters wide) of the 12-story SPSW system were positioned in the middle of the relatively large bays of gravity columns and the nearby 3.2-meter-wide girder bays. Furthermore, in the 20-story SPSW system, the 6.1-meter-wide SPSWs were positioned in the center of the comparatively large bays of neighboring 6.1-meter-wide girder bays and gravity column bays. For 12- and 20-story free-standing SPSW systems, respectively, the wall bay width-to-depth ratio (L/H) is 0.9 and 1.54.

The buildings under examination were a symmetric building situated in Los Angeles, California, on a class D site. It was anticipated that all SPSWs would equally resist the same earthquake loads in both directions by considering the stiff diaphragms of floors and ignoring the torsion effects of structures. Each 12- and 20-story SPSW can therefore withstand one-sixth and one-fourth of the entire seismic load.

The inside (gravity) frames are not included in the two-dimensional (2D) analytical model of the free-standing SPSWs; only the perimeter frames are considered in the SPSW strip. Nonetheless, the P-delta effects resulting from vertical loads tributary to the inner frames, which are transmitted to the SPSW via the stiff floor slab, cannot be disregarded. In the two-dimensional model, an elastic P-delta column

with vertical tributary loads is added as a "lean-on gravity column" (Fig. 4) to transmit the gravity load and consider the P-delta effect from inner frames to the SPSW strip. It is important to note that the leaning columns do not participate in bearing the lateral loads. This column is represented as elements with pin connections at both ends and placed on pinned support on the ground because it solely translates P-Delta effects generated by gravity loads, hence its axial stiffness is infinite, and its moment stiffness is negligible [20]. The pin-ended rigid links that connected the "lean-on gravity column" to the SPSW strip are introduced to transmit loads caused by the mass of the inner frames, see Fig. 7 [21]. A mass proportional is applied with Rayleigh damping of 2% of critical for the first and n^{th} modes, where n is the number of stories.

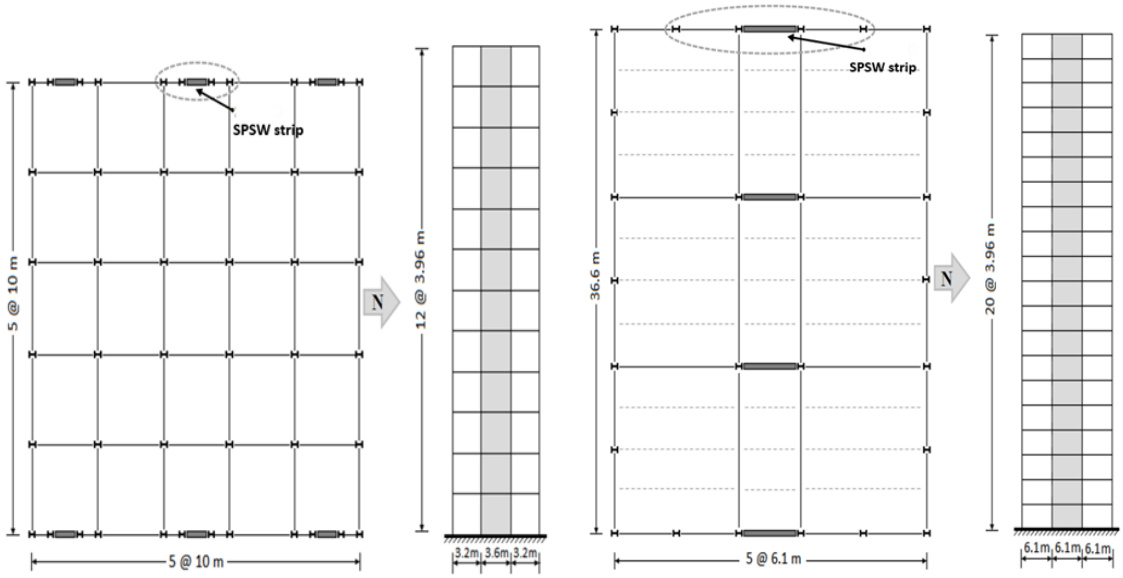

Fig. 3. 12-and 20-story free-standing SPSW Plan view by Meisam et.al. (2017) [13]

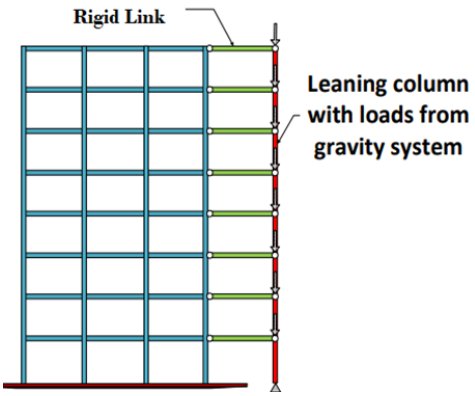

Fig. 4. Illustration of leaning column [21]

3.2 Dual Strip Modeling of SPSW in SAP2000

The shear behavior of unstiffened steel plate shear walls can be modeled analytically using the strip model, which was first put forth by Thorburn and Montgomery (1983) [2] (Fig. 5). The yield drift ratios of the SPSW systems were examined using a number of non-linear response history techniques. The analytical models created for this purpose are dual-strip models that can capture tension field action in both directions as the loading direction changes during earthquakes. The infill plate at each story was divided by fifteen tension-only braced elements hinged at both ends in each loading direction in the

SAP2000 models of the twelve-story buildings. Typically, inelastic analyses of this type set the compression strengths equal to zero, i.e., assuming that the thin infill plates have very little strength in compression.

A well-designed SPSW's initial stiffness and lateral load resistance are mostly unaffected by the strip inclination angle (α), which ranges from 38 to 50 degrees, according to earlier studies [8]. An inclination angle of 42° from the vertical was used to align all of these dual strips. For each of the n strips, the length of the beam segments (Δ_x) is

$$\Delta_x = \frac{1}{n}\,[L + h\ \tan(\alpha)] \tag{1}$$

As defined in the AISC [22], Δ_x is the beam segment's length between nodes, L is the panel's width, h is its height, and n is the strip number. Each strip's area is determined by multiplying the strip width by the plate thickness. For the frame elements and infill plates, ASTM A572 Gr. 50 steel with yield strength (f_y) equals 345 MPa and A36 steel with yield strength (f_y) equals 248 MPa were chosen, respectively. To effectively represent the inelastic behavior of SPSWs and capture the nonlinearity in the models through infill panel yielding, plastic hinges are needed.

At the middle of each strip, lumped axial hinges were added (SAP2000 has multiple hinge models, the Axial-P hinge being one of them). This hinge, like the strips, only takes into consideration yielding brought on by axial stresses. The Fiber P-M2-M3 Hinges, which were modeled using conventional frame components, were put at the potential locations of inelastic deformations in the ends of both VBEs and HBEs [13].

The behavior of the flexural hinges in the beam and column components is shown by user-defined moment against rotation curves, and the behavior of the axial hinges in the tension strips is shown by force against elongation curves. The details of the points (A, B, C, D, and E) of these curves that required definition in SAP2000 are not entirely evident from the verification investigation. Such axial hinges can faithfully replicate the hysteretic tension-only behavior of the strips, as other researchers have confirmed and documented in [23]. Fig. 6 illustrates how we employed the specification of the axial plastic hinge found in [24] after many experiments to arrive at the verification study results.

The Dual-strip models of 12-story Free-Standing SPSWs, generated in SAP2000, are displayed in Fig. 7, respectively. The desired plastic mechanism of the system consists of plastic hinging at the bases of the column (i.e., VBEs and OCs), as well as consistent yielding of the infill plate at the ends of the HBEs. The infill plates and HBEs ends in many stories that start to become plastic as the system yields advances under nonlinear time histories analyses.

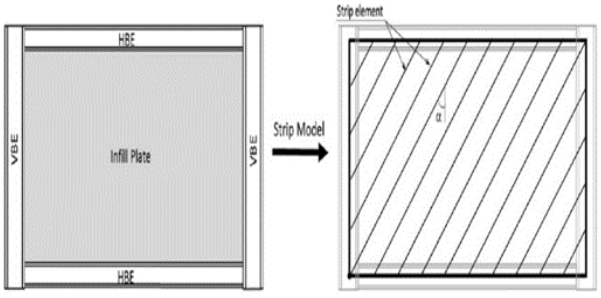

Fig. 5. Strip model representing the SPSW panel [6]

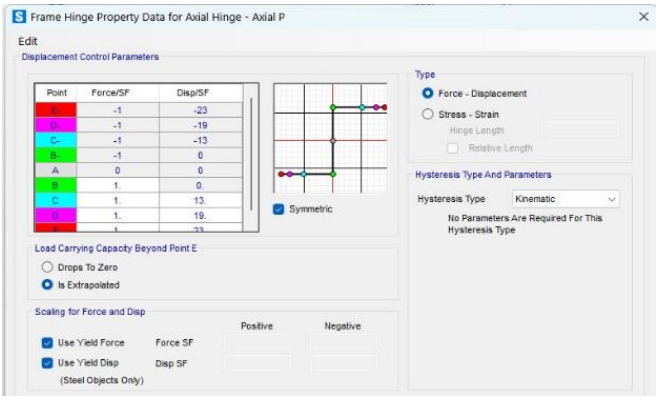

Fig. 6. Bilinear Tension hinge definition in SAP2000 [24]

Two scenarios are taken for the free-standing SPSW, ones when both the OB-to-VBE and OB-to-OC connections are pinned, i.e. the neighboring frames in the SPSW strip potentially offer neither strength nor overturning resistance resulting in a free-standing SPSW, see Fig. 7 [13]. The second considered scenario is when both OB-to-VBE and OB-to-OC are rigidly connected, i.e. participated in SPSW strip strength and overturning resistance, see Fig. 7.

3.3 Nonlinear Dynamic Analysis

A collection of twenty earthquake ground motions (Table 1) that approximate the seismic hazard with a 10% likelihood of surpassing 50 years were used to study the structures nonlinearly. Given that the two most common parameters associated with a seismic event are rupture zone distance (R) and earthquake magnitude (M), it is obvious that identifying these characteristic (M, R) pairings is the easiest selection process. An expanded collection of information is available in the Next Generation Attenuation (NGA) of the PEER database, which is an upgrade and expansion of the PEER strong ground motion data. In ASCE 7–16 [25], the initial time history is scaled by multiplying it by a constant to obtain a scaled time series that either meets or surpasses the target spectrum within a given time frame. The design one-second (SD1) and short-term spectral acceleration parameters (SDS) for the site class were 1.07 g and 0.79 g, respectively, where g is the ground acceleration. Plotting the response spectra for 20 chosen Los Angeles ground motions allows us to validate the records that we obtained from PEER (Fig. 8). The spectral ordinates were matched with those utilized in [21] so that the pre-scaled Los Angeles ground vibrations from the SAC steel project [19] could be used for response history analysis. Assuming a 5% viscous damping ratio, Fig. 9 displays the entire target spectrum for this structure.

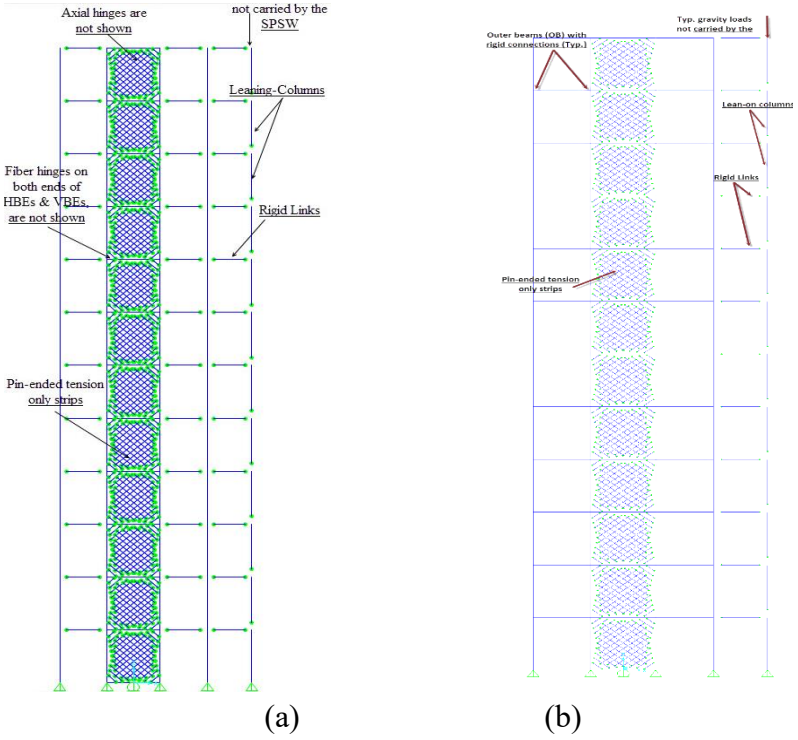

Fig. 7. Dual strip Modelling for Free-Standing SPSW (a) pinned connection of OB to VBE and OC, (b) rigid connection of OB to VBE and OC.

Table 1. Los Angeles ground motions with a probability of exceedance of 10% in 50 years by [13]

Name	Location	Time (sec.)	Magnitude Mw	Peak ground acceleration PGA (cm/sec^2)
LA-01	El Centro 1940 @ Imperial Valley	53.46	6.9	452.03
LA-02		53.46	6.9	662.88
LA-03		39.38	6.5	386.04
LA-04	Imperial Valley, Array#05, 1979	39.38	6.5	478.65
LA-05		39.08	6.5	295.69
LA-06		39.08	6.5	230.08
LA-07		79.98	7.3	412.98
LA-08	Barstow @ Landers, 1992	79.98	7.3	417.49
LA-09		79.98	7.3	509.7
LA-10		79.98	7.3	353.35
LA-11	Gilroy @ Loma Prieta, 1989	39.98	7	652.49
LA-12		39.98	7	950.93
LA-13		59.98	6.7	664.93
LA-14		59.98	6.7	664.49
LA-15	Newhall @ Northridge, 1994	14.95	6.7	523.3
LA-16		14.95	6.7	568.58
LA-17		59.98	6.7	558.43
LA-18		59.98	6.7	801.44
LA-19	Springs, 1986, North Palm	59.98	6	999.43
LA-20		59.98	6	967.61

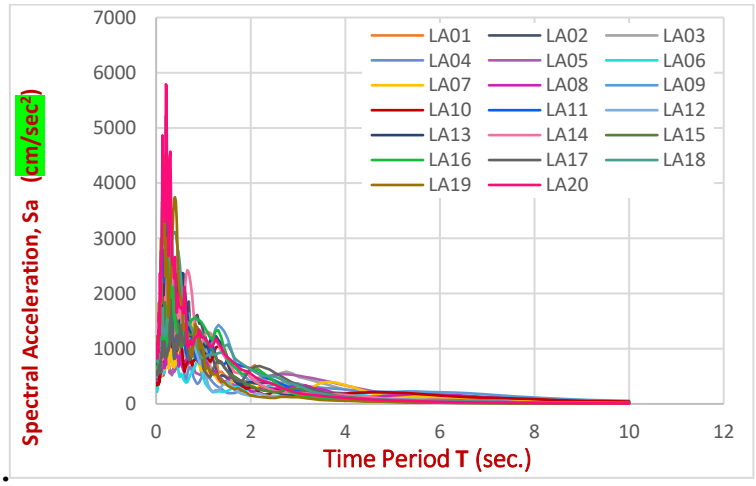

Fig. 8. The elastic 5%-damped Response Spectra for 20 LA Records. by Meisam [13]

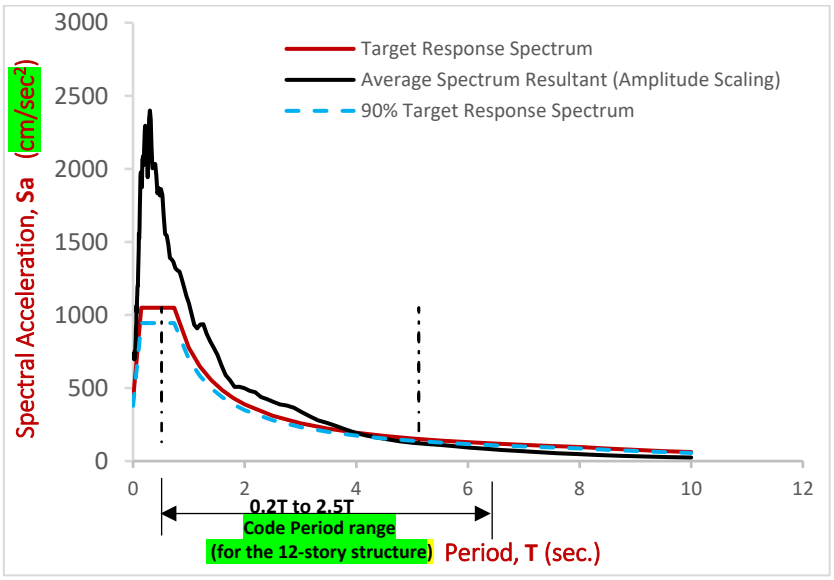

Fig. 9. Design Response Spectra for Los Angeles, California (ζ = 5%) and Average spectrum resultant of the scaled ground motions

3.4 Target Drift Ratio

The target drift ratio, which applies to the degree of damage in the structure, must be determined in the first stage of the design. To protect the structural and nonstructural components from failure, building standards restrict the drifting of design stories. According to the occupancy category and the design's seismic hazard levels, different building standards have different drift limits. Given an earthquake hazard equivalent to 2/3 of the maximum considered earthquake, ASCE-7-16 [25] establishes a 2% drift between stories limit for constructing conventional structures.

3.5 Verification Results and Comparison

From Tables 3 and 5, the fundamental period obtained from the first mode shape of the 12- and 20-story buildings is reported to be 2.56 and 2.87 seconds, respectively when OB and OC elements are pin connected with SPSW with a difference of 0.27% and 1.54% about that obtained from Meisam and Cheng [13]. While the fundamental period of the 12- and 20-story buildings is reported to be 2.22 and 3.513 seconds, respectively when OB and OC elements are rigidly connected with SPSW with a difference of 13.6 % and 20.3% about that obtained from Meisam and Cheng [13].

As illustrated in Tables 2 and 4, the maximum difference between story drift results is 12% for 12- and 20-story buildings when OB elements are pin-connected with SPSW and OC. On the other hand, the difference between story drift results within 39% for a 12-story building and 25% for a 20-story building when OB elements are rigidly connected with SPSW and OC.

Fig. 10 displays the average values of the maximum story drift over the system heights for the 12- and 20-story free-standing SPSWs, based on validated non-linear time history studies of the twenty earthquake motions. Due to the existence of stronger vibration modes, the peak story drifts happened at the top stories; this impact was more pronounced in the free-standing SPSWs. Hence, the pin connection between neighboring columns (VBE and OC) and beams (OB) and SPSW (i.e. the neighboring frames in the SPSW strip potentially offer neither strength nor overturning resistance) is acceptable to use this

model in the parametric study to focus on the efficacy of adding outriggers on the free-standing SPSW system.

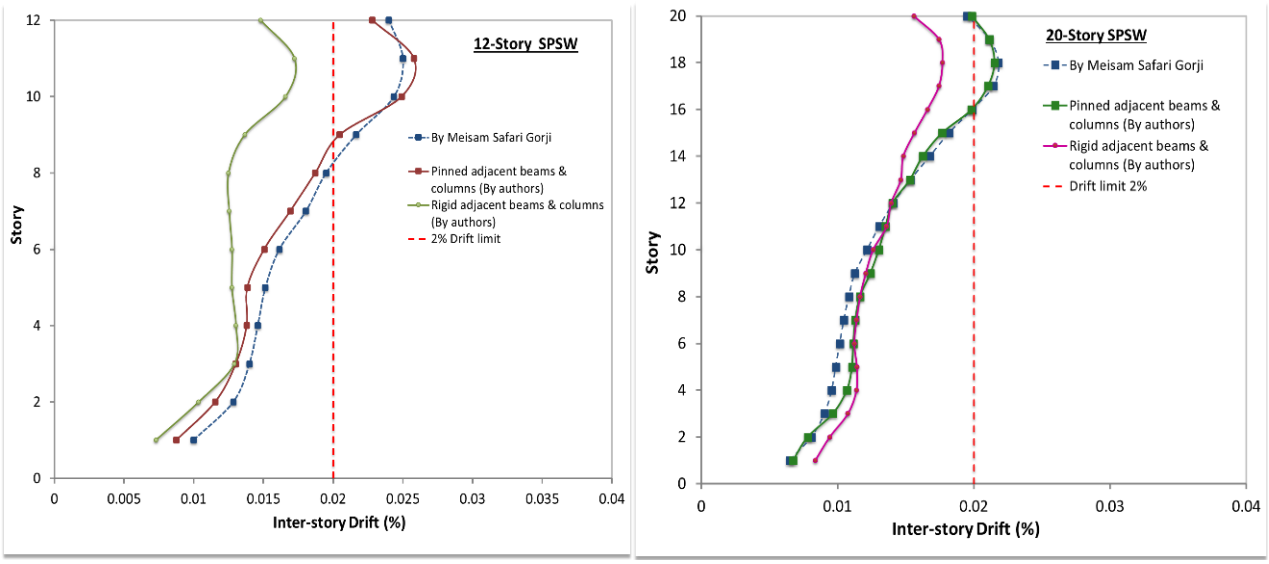

Fig. 10. Comparison of average story drift by Meisam and Cheng [13] and by authors for 12- and 20-story free-standing SPSWs.

Table 1. 12-story Drift Ratio results in comparison for verification.

	Story Drift				
Story	by Meisam and Cheng [13]	Pinned con-nection By authors	Difference %	Rigid connec-tion By authors	Difference %
1	0.0100	0.0088	12%	0.00709	39%
2	0.0128	0.0115	10%	0.01044	24%
3	0.0140	0.0130	7%	0.0133	6%
4	0.0146	0.0138	6%	0.01392	1%
5	0.0151	0.0138	9%	0.01313	3%
6	0.0161	0.0150	7%	0.01289	8%
7	0.0181	0.0170	6%	0.01265	17%
8	0.0195	0.0189	3%	0.01238	24%
9	0.0217	0.0206	5%	0.01336	21%
10	0.0244	0.0249	2%	0.01636	14%
11	0.0250	0.0257	3%	0.01677	7%
12	0.0240	0.0228	5%	0.0138	12%

Table 3. Fundamental periods and mean peak drifts for the 12-story system

	by Meisam and Cheng [13]	Pinned connection	Difference %	Rigid connection	Difference %
		By authors		By authors	
Period (sec.)	2.57	2.563	0.27%	2.22	13.6%
Story Drift	0.025	0.0257	2.8%	0.01723	31%
Top Drift	0.0157	0.017	8.3%	0.013	17.2%

Table 4. 20-story Drift Ratio results in comparison for verification.

	Story Drift				
Story	by Meisam and Cheng [13]	Pinned connection by authors	Difference %	Rigid connection by authors	Difference %
1	0.0065	0.0067	4%	0.0081	25%
2	0.0081	0.0078	3%	0.0093	16%
3	0.0091	0.0097	7%	0.01105	22%
4	0.0096	0.0107	12%	0.0117	23%
5	0.0099	0.0111	12%	0.01176	19%
6	0.0102	0.0112	10%	0.01153	13%
7	0.0105	0.0113	8%	0.01152	10%
8	0.0108	0.0116	7%	0.01156	7%
9	0.0113	0.0124	10%	0.01175	4%
10	0.0122	0.0130	7%	0.01215	0%
11	0.0131	0.0135	4%	0.0129	1%
12	0.0141	0.0140	0%	0.0134	5%
13	0.0154	0.0153	0%	0.01448	6%
14	0.0168	0.0163	3%	0.01534	8%
15	0.0182	0.0177	3%	0.01645	9%
16	0.0199	0.0198	0%	0.017375	13%
17	0.0214	0.0210	2%	0.018048	16%
18	0.0218	0.0215	1%	0.01813	17%
19	0.0211	0.0211	0%	0.017749	16%
20	0.0195	0.0199	2%	0.01596	18%

Table 5. Fundamental periods and mean peak drifts for the 20-story system

	by Meisam and Cheng. [13]	Pinned connection	Difference %	Rigid connection	Difference %
		By authors		By authors	
Period (sec.)	2.92	2.875	1.54%	3.513	20.3%
Story Drift	0.0218	0.0215	1.4%	0.01744	20%
Top Drift	0.012	0.01428	19%	0.01353	12.75%

4 Definition of Buckling Restrained Brace (BRB) Outrigger System

Outriggers are frequently employed for increasing the lateral stiffness and decreasing the lateral displacement of tall, slender buildings where the over-turning moment is strong relative to base shear. This paper suggests replacing the standard diagonal bracing in mid- or high-rise steel plate shear walls with energy-dissipating outrigger trusses installed using buckling restrained braces (BRBs). This will improve the seismic performance of the outrigger (BRB-O), in which the BRBs' inelastic responses dissipate some of the seismic energy. The BRB frames produce a symmetric hysteretic response by increasing compressive capacity while retaining tensile strength.

Tensile capacity is provided by the ductile steel core of a standard BRB, which is intended to yield under compression and tension. The steel core is contained inside a steel casing before being filled with mortar or concrete [26] (as indicated in Fig. 11) to prevent the steel component from buckling under compressive force. Before the mortar is cast, an unbinding substance or very small air gap is left between the mortar and the steel core to prevent normal force transfer from the steel core to the surrounding mortar and hollow structural section components of BRB. Because of this, unlike conventional bracing, the core in BRB may absorb energy and experience significant yielding under both tension and compression.

4.1 Modeling of BRB system

Low-yield-point (LYP) materials can be utilized in place of typical structural steel grades such as A36 to achieve early yielding in members [19]. The nominal yield strength, f_y, of the steel used to make the dissipative core of the BRBs is 248 MPa, and it is grade ASTM A36. The BRB backbone curve's behavior during the design phase is described in detail in Fig. 12. For the BRB modeling in SAP2000, a multilinear plastic link element with BRB hysteresis type was utilized (Fig. 12). Since it is expected that the BRB steel core will withstand the whole axial load in the outrigger elements, the yielding limit state was used in calculating the necessary cross-section area of the steel core, or A_{sc}. Therefore, Eq. (2) can be used to determine the design axial force strength of the BRB, P_{ysc}.

According to the seismic provisions AISC341-16 [5]. The adjusted brace strength in tension shall be, P_{nt}, and the adjusted brace strength in compression shall be P_{nc}, which are calculated by equations (3) and (4), where β, the modification coefficient for strength in compression, was set at 1.1 in this study; ω, the strain hardening modification coefficient, was taken equal to 1.25; and R_y, the ratio between the expected and nominal yield strengths, was taken as 1.1. Assuming that the BRB yield length represents

70% of the overall length, the backbone curve of the BRB was created using the strength, area, and stiffness data [16]. It was expected that the post-yielding stiffness K_f in tension would be 1.5% of the original stiffness K_0, as determined by Eq. (5). If the yield deformation is computed using Equation (6), where E = 29,000 ksi, and L is 70% of the brace length.

$$P_{ysc}=F_y A_{sc} \quad (2)$$

$$P_{nt}=\omega R_y P_{ysc} \quad (3)$$

$$P_{nc}=\beta \omega R_y P_{ysc} \quad (4)$$

$$K_0=\frac{E A_{sc}}{L} \quad (5)$$

$$\Delta_y=\frac{\sigma}{E}*L \quad (6)$$

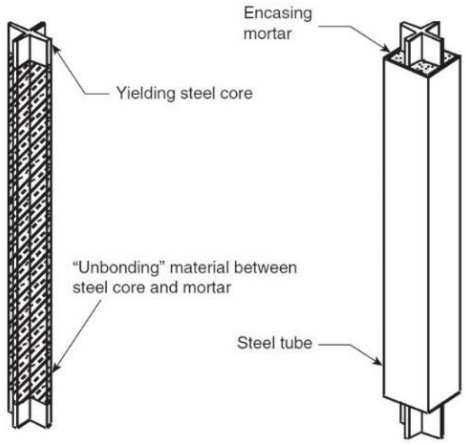

Fig. 11. Components of a BRB element [17]

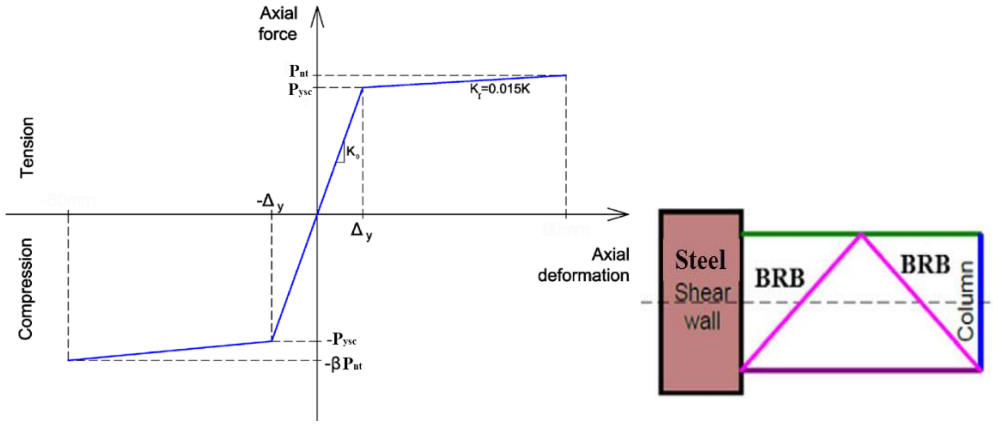

Fig. 12. BRB Backbone Curve [5] and the used Outrigger Configuration

Utilizing ETABS software, which includes definitions for different BRB frame element shapes such as Star Seismic BRB which was used in this study, and the verified free-standing SPSW model with the same designed frame sections in the parametric study. Appropriate Star Seismic BRB sections are chosen and defined in SAP2000 V24.0.1 [28] as a multilinear plastic link, as illustrated in Fig. 13 all BRB

elements defined to be pinned ended with deformation direction U1. A comparison between experimental full-scale brace testing and numerical modeling (using the multilinear link created in SAP2000) Findings were developed in [27], with the multi-linear model exhibiting behavior that was comparable to the experimental model. As indicated in Tables 6, 7, and Fig. 13, the design of BRB-O truss elements incorporates two distinct sizes for the steel core of the BRB-Os. The larger section is utilized in the position that requires a dissipated energy element and has a high seismic response for all models. It is noteworthy to mention that the linear effective damping for nonlinear Link/Support elements was not used for nonlinear direct-integration time history analysis in the model [28] to prevent unreasonably large, damped force in the location in the linked beam.

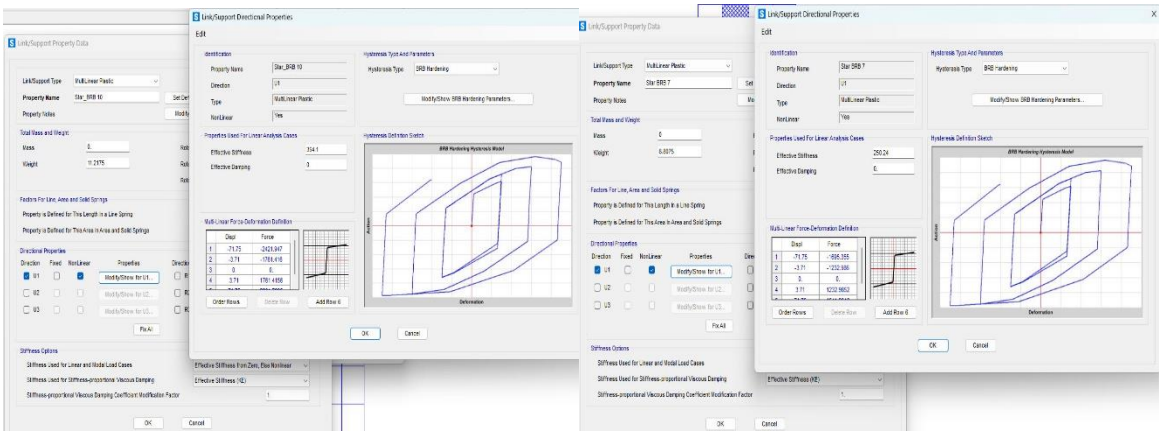

(a) **(b)**

Fig. 13. Definition of (a) BRB-O (starBRB10), and (b) BRB-O (starBRB7) elements in SAP2000 12-story SPSW system

Table 6. Selected Buckling-restrained braces: size, and Strength for the 12- and 20-story SPSW

BRB cross-section	Star-BRB_10	StarBRB_7
Area of steel core, Asc [mm^2]	6451.6	4516.1
Ultimate axial tension force, P_{max} [kN]	2201.77	1541.2318
Ultimate axial compression force, βP_{max} [kN]	-2421.947	-1695.355

Table 7. Selected Buckling-restrained Braces: Yield, and Ultimate Deformation According to Their Steel Core Yield Length

Story	Steel core yield length L_y[mm]	Initial stiffness, K_0[kN /mm]		Yield deformation, Δ_y[mm]	Ultimate deformation, Δ_u[mm]
		Star-BRB_10	Star-BRB_7		
20-Story	3499	368.672	258.07	4.3386	83.9442
12-Story	2989.7	431.474	302.03	3.707	71.75

4.2 Case of Studies

The same characteristics of the finite element models represented in the verification models are used to investigate the effect of the buckling restrained brace outrigger (BRB-O) on enhancing the overturning stiffness of the unstiffened steel plate shear wall (SPSW). Parameters subject to investigation included single and double BRB-O truss elements, added to various locations in the structure, and the wall panel width-to-depth ratio with different structure heights (mid- and high-rise SPSWs). An optimum location of BRB-O is being developed to make this technology economic [29]. This research [29] reached the result that placing an outrigger at a height where the h/H ratio is lower than 0.2 reduces the efficiency of a minimum. Therefore, we start adding a single (one) BRB-O truss from the 3rd story.
Thirty SPSW with BRB outriggers (SPSW-BRB-O) finite element models with various geometric parameters were modeled and analyzed using SAP 2000. The models represent three sets of scenarios to be analyzed for both 12- and 20-story SPSWs with various locations of the BRB-O. Firstly, the single BRB-O in the 1/3, 1/4, 1/2, 2/3, 3/4 H, and the top story. Secondly, the double BRB-O is divided into two groups of scenarios; these scenarios are different combinations of the positions that a pair of outriggers can take along the structure as listed in Table 7.

Table 7. 12- and 20-Story Studied Models

No.	Model	12- story building		20- story building	
		Location of BRB	Floor with BRB	Location of BRB	Floor with BRB
1	No BRB	-	-	-	-
2	Single BRB-O	1/3 H	4th	1/3 H	7th
3		1/2 H	6th	1/2 H	10th
4		2/3 H	8th	2/3 H	13th
5		3/4 H	9th	3/4 H	15th
6		H	12th	H	20th
7	Double BRB-O (1)	1/4 H & 1/2 H	3rd &6th	1/4 H & 3/4 H	5th & 15th
8		1/4 H & 3/4 H	3rd &9th	1/3 H & 3/4 H	7th & 15th
9		1/3 H & 3/4 H	4th &9th	1/3 H & 2/3 H	7th & 13th
10		1/2 H & 3/4 H	6th &9th	1/2 H & 3/4 H	10th & 15th
11		1/3 H & 2/3 H	4th & 8th	1/4 H & 1/2 H	5th & 10th
12	Double BRB-O (2)	1/3 H & H	4th & 12th	1/3 H & H	7th & 20th
13		1/2 H & H	6th & 12th	1/2 H & H	10th & 20th
14		2/3 H & H	8th & 12th	2/3 H & H	13th & 20th
15		3/4 H & H	9th & 12th	3/4 H & H	15th & 20th

5 Results and discussion

The next sections present the nonlinear dynamic time history analysis findings for three distinct position scenarios. To establish the ideal location, the impact of the outrigger position on seismic demand is ascertained. It should be mentioned that the mean values of various seismic parameters for seismic motions with 10% hazard levels in 50 years are displayed in all computations and graphics.

5.1 Time-period

The fundamental periods obtained from all models are detailed in Table 8. Using BRB-O trusses either single or double led to shortening the time-period in mid-rise SPSW buildings more than high-rise SPSW buildings by about 3%. This is due to more stiffness of used BRB-O rising from shorter length of the steel core of BRB-O members in mid-rise building.

For single BRB-O in both mid-rise and high-rise SPSW buildings, higher leveling of added outrigger from the ground level led to more reduction in time-period i.e. buildings become stiffer, except in the case of added outrigger at roof level. The single BRB-O truss indicates that adding the outrigger truss to both mid-rise and high-rise SPSW buildings at (3/4 H) resulted in the lowest period, making it the best position. The second outrigger was added, which increased the structure's stiffness. The fundamental period of vibration and structural stiffness is altered when the second outrigger is moved along the structure's height.

For 12-story SPSWs with single BRB-O at 3/4 H, and with double BRB-Os at 1/2 H & 3/4 H and BRB-O @ 2/3 H & H, the reduction in fundamental periods results in 16%, 20%, and 19%, respectively of the free-standing SPSW. In addition, for 20-story SPSWs, the reduction ratios are 13%, 18%, and 16% for the models with single BRB-O at the 3/4 H, and with double BRB-Os at the 1/2 H & 3/4 H and BRB-O @ 2/3 H & H, respectively. Therefore, in both mid- and high-rise SPSW buildings, it is preferred to add BRB-O above 2/3 of the SPSW height.

5.2 Story Lateral Displacement

The mean story displacements for all 12- and 20-story models from nonlinear response analyses of 20 earthquake ground motions are shown in Fig. 14. As it is illustrated, by adding a single BRB-O the story displacements decrease in comparison to the free-standing SPSW. All models behave very closely to each other, and the lowest value is obtained from the one in which the BRB-O is added in the 9^{th} and 15^{th} stories (3/4 H) by about 20% in 12-story systems and 10% in 20-story systems. Higher leveling of the added outrigger from the ground level led to more reduction in lateral displacement. Subsequently, the lateral displacement dropping is increased by adding a double inter-story BRB-Os, which is clearly what happened in the model of SPSW with double BRB-Os at the 4^{th} & 9^{th} stories (1/3 H & 3/4 H) in the 12-story system by about 27% and 10^{th} & 15^{th} stories (1/2 H & 3/4 H) in the 20-story systems by about 15% with the lowest lateral displacement (Table 9 & 10). The lowest lateral displacement occurs in position (3/4 H & TOP stories) for both 12- and 20-story systems when adding top BRB-O conjugated to inter-story BRB-O by about 29% in 12-story systems and 17% in 20-story systems. There was a greater reduction in lateral displacement with higher leveling of the additional inter-story BRB-O coupled to the top BRB-O from the bottom level.

5.3 Inter-story Drift Ratio

In Fig. 15, simplified mean inter-story drift graphs for the SPSW with single BRB-O and Double BRB-Os models from nonlinear response analyses of 20 earthquake ground motions are presented, and the comparison of the dissipated outriggers effect on the SPSWs is studied, and illustrated in Tables 10 and 11. Since the outrigger stiffens that tale, it is clear from all graphs that the drift ratio changes abruptly at the BRB-O location. The maximum drift ratio difference in the SPSW with BRB-O systems is observed at the 9^{th}, 4^{th} & 9^{th}, and 9^{th} & top floors in the 12-story SPSW with single and double BRB-O

trusses, respectively, and at the 15th, 10th & 15th and 15th and top floors of the 20- story SPSW with single and double BRB-O trusses, respectively.

Table 8. 12- and 20-story SPSWs with BRB-Os Fundamental Time-Periods (sec.)

Model		Period (Sec.)		Reduction ratio	
		12-story	20-story	12-story	20-story
Free-standing SPSW (no outrigger)		2.56	3.79	-	-
Single BRB-O	BRB-O@ 1/3 H	2.34	3.56	9%	6%
	BRB-O @ 1/2 H	2.22277	3.39	13%	10%
	BRB-O @ 2/3 H	2.15502	3.303	16%	13%
	BRB-O @ 3/4 H	2.15427	3.299	**16%**	**13%**
	BRB-O @ H	2.26242	3.50	12%	8%
Double BRB-O (1)	BRB-O @ 1/4 H & 1/2 H	2.17338	3.30	15%	13%
	BRB-O @ 1/4 H & 3/4 H	2.09548	3.20	18%	15%
	BRB-O @ 1/3 H & 3/4 H	2.0709	3.15	19%	17%
	BRB-O @ 1/2 H & 3/4 H	2.04807	3.11	**20%**	**18%**
	BRB-O @ 1/3 H & 2/3 H	2.07815	3.17	19%	16%
Double BRB-O (2)	BRB-O @ 1/3 H & H	2.14134	3.29	16%	13%
	BRB-O @ 1/2 H & H	2.08584	3.20	19%	15%
	BRB-O @ 2/3 H & H	**2.0775**	**3.18**	**19%**	**16%**
	BRB-O @ 3/4 H & H	2.09642	3.22	18%	15%

The inter-story drift ratios become more non-uniform as the number of BRB-O trusses increases (double trusses instead of single ones). In the 12-story SPSW, the maximum story drifts at upper stories exceeded the 2% drift limit, the same in both SPSW systems with single and double BRB-O, except the models including BRB-O at 9th, 4th with 9th, and 9th & top, with a maximum of 1.94%, 1.88%, and 1.83%, respectively. For the 20-story SPSW with BRB-O systems, it is observed the lowest mean drift ratio at the 15th story, at the 10th & 15th stories for double BRB-O trusses, in case of scenario (1), and at the 15th & top stories for double BRB-O trusses, in case of scenario (2), with a maximum drift ratio of 1.75%, 1.66%, and 1.44%, respectively.

As inter-story drift is a crucial engineering parameter rather than roof displacement for mid- and high-rise buildings, therefore, we have determined the optimal locations for the BRB-O truss in both 12- and 20-story SPSWs from the three sets. Installing a single BRB outrigger in the stories near the middle height is more effective in improving SPSW stiffness than installing one in the top story, especially when it is placed at 3/4 of the structure's height, despite the high level of lateral displacement and inter-

story drift ratio in the upper stories of the SPSW. There was a greater decrease in inter-story drift with higher leveling of the outrigger from the ground level.

Even more so than with a single BRB-O truss, the drift ratio can be decreased to be less than its code limit by adding a double truss. The best part is that this can be done without raising the truss section profile, which reduces the weight of the structure and increases its economy. Positioning the double BRB outriggers; one at the top and the other at the high level of the structure's height; is most efficient, especially when the other outrigger is at 3/4 of the structure's height. When the second inter-story BRB-O attached to the top BRB-O from the bottom level was leveled higher, there was a greater reduction in inter-story drift. Adding the double BRB outriggers where one of them is at the top story is more efficient than adding the double BRB outriggers between inter-stories.

Table 9. 12-story SPSW with BRB-O Peak story response in terms of displacement and drift

	Model configurations	**Mean top displacement (mm)**	**Reduction ratio**	**Mean story drift**	**Reduction ratio**
Free-standing SPSW (no BRB outrigger)		814.7	-	0.0257	-
Single BRB	BRB-O@ 1/3 H	719.342	11.7%	0.0247	3.9%
	BRB-O @ 1/2 H	685.286	15.9%	0.0238	7.4%
	BRB-O @ 2/3H	664.241	18.5%	0.0219	14.8%
	BRB-O @ 3/4 H	652.104	20.0%	0.0194	24.5%
	BRB-O @ H	682.888	16.2%	0.0221	14.0%
Double BRB (1)	BRB-O at the 1/4H & 1/2 H	634.837	22.1%	0.0230	10.4%
	BRB-O at the 1/4 H & 3/4 H	598.206	26.6%	0.0188	26.6%
	BRB-O at the 1/3H & 3/4 H	590.96	27.5%	0.0189	26.5%
	BRB-O at the 1/2H & 3/4 H	592.96	27.2%	0.0189	26.3%
	BRB-O at the 1/3H & 2/3H	608.496	25.3%	0.0214	16.4%
Double BRB (2)	BRB-O at the 1/3 H & TOP	609.639	25.2%	0.0207	19.3%
	BRB-O at the 1/2 H & TOP	590.03	27.6%	0.020	22.1%
	BRB-O at the 2/3 H & TOP	591.47	27.4%	0.0183	28.8%
	BRB-O at the 3/4 H & TOP	576.41	29.2%	0.0171	33.5%

Table 10. 20-story SPSW with BRB-O Peak story response in terms of displacement and drift

	Model configurations	Mean top displace-ment (mm)	Re-duction ratio	Mean story drift	Reduc-tion ratio
Free-standing SPSW (no BRB outrigger)		1131.1	-	0.0257	-
Single BRB	BRB-O@ 1/3H	1091.885	3.6%	0.02110873	3%
	BRB-O @ 1/2H	1072.875	5.4%	0.020541065	6%
	BRB-O @ 2/3H	1049.654	7.8%	0.019528951	12%
	BRB-O @ 3/4H	1022.584	10.6%	0.0174912	26%
	BRB-O @ H	1005.105	12.5%	0.0171938	18%
Double BRB (1)	BRB-O at the 1/4 H & 1/2 H	1034.407	9.3%	0.0194067	12%
	BRB-O at the 1/4 H & 3/4 H	1005.375	12.5%	0.0174913	25%
	BRB-O at the 1/3 H & 3/4 H	992.802	13.9%	0.0171138	27%
	BRB-O at the 1/2 H & 3/4 H	985.702	14.8%	0.0166584	31%
	BRB-O at the 1/3 H & 2/3H	1005.079	12.5%	0.0180950	20%
Double BRB (2)	BRB-O at the 1/3 H & TOP	609.639	14.9%	0.0163562	33%
	BRB-O at the 1/2 H & TOP	969.997	10.6%	0.0155943	40%
	BRB-O at the 2/3 H & TOP	962.916	9.0%	0.0148	47%
	BRB-O at the 3/4 H & TOP	970.4707	16.6%	0.01438	52%

5.4 VBEs Demands

One of the important advantages of the outrigger is the reduction of overturning moment on the lateral system and the axial forces in the inner columns. The mean maximum axial forces at the base of the vertical boundary elements (VBEs) from nonlinear time history analyses are extracted and illustrated in Fig. 21. In mid-rise SPSWs with BRB-Os, it has been observed that the highest axial force reduction ratio occurs when there's one BRB-O at the 9th story (3/4 H) by 20.9%. Additionally, in the case of the double BRB-O, the reduction ratio increases as the position comes closer to the base, such as at the 1/4 & 1/2 H by 25.6%, and the 1/3 H & top story by 24.7%. When using BRB-Os in high-rise SPSWs, there is a minor axial force reduction for VBEs. The maximum axial force reduction ratio has been found to happen when there is a single BRB-O at 1/3 H by 5.3%. Furthermore, the reduction in the ratio increases in the double BRB-O scenario as the position becomes closer to the base, for example, by 3.7% at the

1/3 H & top story and 6.6% at the 1/4 & 1/2 H. Therefore, the efficiency of adding BRB as outriggers is diminished for high-rise SPSW buildings.

There is a difference in VBEs axial force reduction between adding a single BRB-O and double BRB-O, which ranged from about 21-26% for mid-rise SPSW buildings and 4-7% for high-rise SPSW buildings. The minimal effect on axial force reduction in VBEs single BRB-O and double BRB-O appeared in high-rise SPSW buildings due to using longer BRB-O members (lower stiffness of BRB-O) and wider SPSW system (with larger L/H of wall panel).

It is worth noting in Table 12 that when the width-to-depth (L/H) ratio of the web panel increases in the 20-story SPSW, it affects the reduction in the VBEs axial forces, which is diligently lower than in the wide 20-story wall due to the larger bending moment arm. In addition, its axial forces increase after adding the BRB outrigger at the top story (roof). Adding an outrigger truss at the top story is not recommended in such cases, whether single or double outrigger trusses.

The length of the BRB core yield affects the reduction ratio of the VBEs axial force. In the case of 12-story SPSWs with BRB-O, the outrigger width is smaller in comparison to the 20-story models. Consequently, the BRB core length in the 12-story structures is also smaller, significantly impacting its stiffness. We have demonstrated the advantages of shortening the yielding portion to improve structural efficiency. This results in higher axial stiffness, reduced weight, a more adaptable design, and simplified restraint mechanisms.

Table 11. Mean maximum axial forces of the VBEs for 12- and 20-story SPSWs with BRB-Os, at various positions

Cases	Model configurations	Mean maximum VBEs axial forces (kN)		Reduction ratio	
		12-story	20-story	12-story	20-story
12-story Free-standing SPSW (no BRB outrigger)		38898.84	36381.46	-	-
Single BRB	BRB-O@ 1/3H	32008.35	34450.91	17.7%	5.3%
	BRB-O @ 1/2H	32071.12	34966.12	17.6%	3.9%
	BRB-O @ 2/3H	31052.97	35611.16	20.2%	2.1%
	BRB-O @ 3/4H	30770.99	35656.65	20.9%	2.0%
	BRB-O @ H	33586.96	37072.93	13.7%	-1.9%
Double BRB (1)	BRB-O at the 1/4 H & 1/2 H	28937	33988.62	25.6%	6.6%
	BRB-O at the 1/4 H & 3/4 H	30556.9	34594.28	21.4%	4.9%
	BRB-O at the 1/3 H & 3/4 H	29114.6	34656.42	25.2%	4.7%
	BRB-O at the 1/2 H & 3/4 H	29142.3	35567.05	25.1%	2.2%
	BRB-O at the 1/3 H & 2/3 H	29238.5	34656.42	24.8%	4.7%
Double BRB (2)	BRB-O at the 1/3 H & TOP	29297.35	35034.28	24.7%	3.7%
	BRB-O at the 1/2 H & TOP	29596.95	35875.43	23.9%	1.4%
	BRB-O at the 2/3 H & TOP	30733.12	36756.64	21.0%	-1.0%
	BRB-O at the 3/4 H & TOP	30210.54	37100.67	22.3%	-2.0%

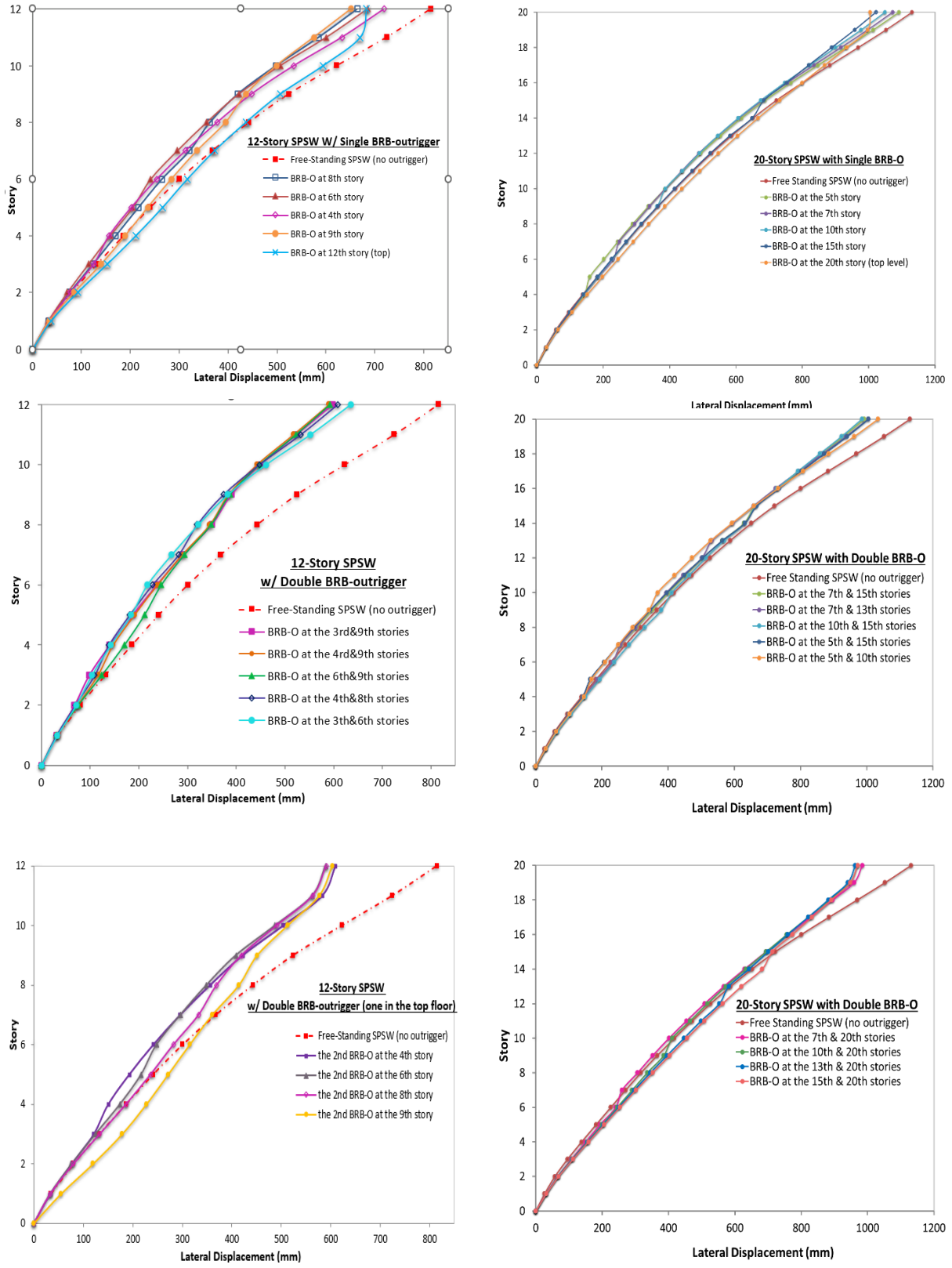

Fig. 14. Mean Peak Story displacements for 12- and 20-story SPSWs with BRB Outriggers in various locations

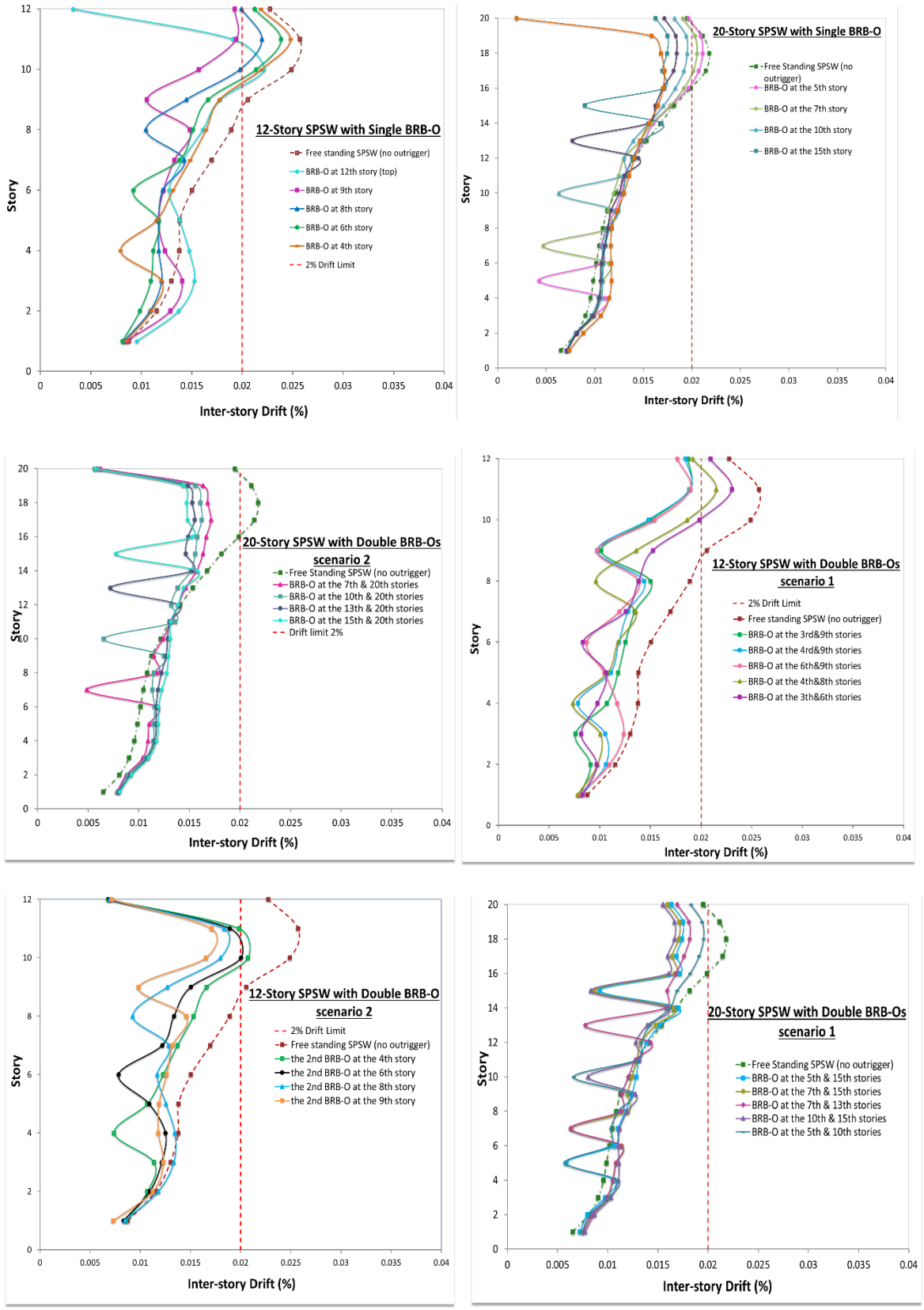

Fig. 15. Comparisons of the Inter-story Drift ratios for 12-story SPSWs with and without BRB-O

5.6.Cost-effectiveness and Practicality of Implementing of SPSW-BRB-O System.

The primary factors analyzed in these comparisons were material cost and detailing cost of link-column connection. Material cost was computed by multiplying the unit weight of steel beams, the length of the member, and the steel unit price. Based on the steel core area and length, BRB prices were interpolated. The steel fabricator estimate was used to compute the welding cost. A fixed cost per weld (weld prep and erection bolts) and the cost of full joint penetration welds were included in the estimate. While the improved seismic performance frequently justifies the increased cost of the system, the fabrication costs associated with the Buckling-restrained braces (BRB) and the connections used in such a system between BRB members and SPSW, would likely outweigh the savings in steel weight and could potentially be deterrent to system use.

Reductions in the axial forces in the VBE columns of the SPSW, when BRB-O was added, resulted in a decrease in the necessary cross sections of the SPSW VBE columns, which in turn led to a decrease in the total weight.

For high-rise SPSW buildings, the effectiveness of using BRB as outriggers is reduced due to minimal reduction in VBEs axial force compared to mid-rise SPSW buildings. In mid-rise or high-rise SPSW structures, increasing the number of BRB-O from single to double has a slight effect on the axial force of the VBEs, i.e. increasing the number of BRB-O has no enhancing effect. The axial stiffness of BRB (Buckling Restrained Brace) members decreases when their steel core is lengthened, reducing their effectiveness in reducing the axial forces of VBEs. Also, increasing the length of the steel core of BRB members lead to higher costs. Therefore, shorter BRBs are preferred to save money and improve efficiency.

6 Conclusions

This study proposes a new Steel Plate Shear wall with buckling restrained braces outrigger (BRB-O) truss as an energy-dissipation system. A case study combining dynamic time history analysis and comparing the new structure's seismic reactions with the different heights of free-standing SPSWs under 20 pairs of earthquakes with varying intensities confirmed the new SPSW's seismic performance. The following are the primary conclusions:

1. The lateral behavior of the SPSW under earthquake load is significantly influenced by the location and number of the outrigger trusses more than its strength, so the best outrigger locations for the building must be carefully chosen during the building design. Consequently, it reduces the increase in the BRB cross-sectional area, so decreasing the desirable additional weight.

2. In the design of tall structures, it is important to consider lateral displacement and drift. Research shows that placing a single BRB outrigger near the middle of a SPSW improves SPSW stiffness, especially when positioned at 3/4 of the structure's height. For double outriggers, placing one at 3/4 of the structure's height or at the top, and placing the second near the mid-height, significantly enhances the structure's stiffness. This arrangement fulfills the criteria for inter-story drift ratio across various seismic conditions.

3. Adding a single (one) BRB-O at the top story (the roof) is ineffective in energy dissipation of the seismic loads. This affects the reduction of the VBEs' axial force demands, especially in the high-rise SPSW.

4. Raising the single BRB-O to a higher level from the ground resulted in a significant decrease in inter-story drift and lateral displacement. When two BRB-Os were used, a higher level for the second inter-story BRB-O from the bottom level added to the top BRB-O resulted in a greater reduction in lateral displacement and inter-story drift. This is because when the levels of inter-story BRB-Os increase, the SPSW with BRB-O systems become stiffer.

5. The width-to-depth (L/H) ratio of the wall web panel affects the reduction in the VBE's axial forces. This reduction is considerably lower in the wide SPSW (with $L/H \geq 1.5$) compared to the narrow SPSW (with $L/H \leq 1$). As a result, the reduction in VBE axial demands leads to decreased required cross-sections, which in turn increases the lateral system economy and the usable interior space of the building.

6. The length of BRB steel cores plays a significant role, particularly when it is reduced. They demonstrate exceptional performance in terms of initial stiffness, ultimate strength, and energy dissipation capacity.

7. Due to the use of longer BRB-O members (which have lower BRB-O stiffness) and a wider SPSW system (which has greater L/H of wall panels), the axial force reduction in VBEs single BRB-O and double BRB-O had a minimal impact (about 4-7%) on high-rise SPSW buildings.

7 Future Research Works

- Weight comparison of the SPSWs can be carried out after redesigning its components, to determine the impact of different outrigger types and numbers and locations on the overall building weight, including free-standing SPSW, SPSW with BRB outrigger, and compared with conventional outrigger truss.
- This study focused on the effect of buckling restrained braces as outriggers (BRB-Os) in free-standing SPSW systems. More FE models are recommended to include the full stiffness contribution of beams and columns adjacent to the SPSW system in cases with BRB-Os.
- The buckling restrained brace has many shapes of steel core cross-sections, which may affect its seismic behavior. The most common shapes and types of BRB, according to the manufacturer, are core brace BRB and star seismic BRB [18]. In addition to their connection type, bolted lug, welded or pinned. All these parameters need to be studied through more FE models.
- Represent the structure in 3D models by applying the two components of each ground motion in their respective directions, instead of analyzing the entire time history in 2D.
- Experimental studies of the SPSW prototype with buckling restrained brace outrigger (BRB-Os) under artificial lateral or cyclic loading.

References

1. Majlesi, A., Asadi-Ghoozhdi, H., Bamshad, O., Attarnejad, R., Masoodi, A. R., and Ghassemieh, M., "On the Seismic Evaluation of Steel Frames Laterally Braced with Perforated Steel Plate Shear Walls Considering Semi-Rigid Connections," Buildings, vol. 12, no. 9. 2022. doi: 10.3390/buildings12091427.
2. Thorburn LJ, Montgomery CJ, K. G., "Analysis of Steel Plate Shear Walls," Structural engineering report SER 107 | SER-ID SER107, pp. 549–554, 1983, doi: 10.3850/978-981-08-6218-3_ss-we025.
3. Roberts, T. M., and Sabouri Ghomi, S., "Hysteretic characteristics of unstiffened plate shear panels," Thin-Walled Struct., vol. 12, no. 2, pp. 163–174, 1991, doi: 10.1016/0263-8231(91)90062-N.
4. Jeffrey W. Berman, M. B., "Experimental investigation of light-gauge steel plate shear walls," J. Struct. Eng., vol. 190, no. February, pp. 259–267, 2005, doi: 10.1016/j.jcsr.2022.107138.
5. AISC 341-16 - American Institute of Steel Construction, "Seismic Provisions for Structural Steel Buildings," Seism. Provisions Struct. Steel Build., no. 1, p. 402, 2016.
6. Vasseghi, A., and Khoshkalam, V., "Effect of Outrigger Panels on Seismic Performance of Steel Plate Shear Wall Structural System," Int. J. Steel Struct., vol. 20, no. 4, pp. 1180–1192, 2020, doi: 10.1007/s13296-020-00350-4.
7. Bakhshi H., Khosravi H., and Ghoddusi M., "Evaluation of Seismic Behavior of Steel Shear Wall by Time History Analysis," Journal of Computational Engineering and Physical Modeling vol. 2 - issue 1 (2019) 38-55. doi: 10.22115/CEPM.2019.160278.1055.
8. Alinia, M.M. and Dastfan, M., "The effects of surrounding members on post-buckling behaviour of thin steel plate shear walls (TSPSW)," Fourth Int. Conf. Adv. Steel Struct., Elsevier; 2005, p. 1427–32. doi:10.1016/B978-008044637-0/50212-2.
9. Alinia, M.M. and Dastfan, M., "Behaviour of thin steel plate shear walls regarding frame members," J Constr Steel Res 2006;62:730–8. doi: 10.1016/j.jcsr.2005.11.007.
10. Berman, J. W., and Bruneau, M., "Capacity design of vertical boundary elements in steel plate shear walls," Eng. J., vol. 45, no. 1, pp. 57–71, 2008, doi: 10.62913/engj. v45i1.925.
11. Qu, B., and Bruneau, M., "Design of steel plate shear walls considering boundary frame moment resisting action," 9th US Natl. 10th Can. Conf. Earthq. Eng. 2010, Incl. Pap. from 4th Int. Tsunami Symp., vol. 5, no. December, pp. 4066–4075, 2009, doi: 10.1061/(asce)st.1943-541x.0000069.
12. Moghimi, H., and Driver, R. G., "Performance-Based Capacity Design of Steel Plate Shear Walls. I: Development Principles," J. Struct. Eng., vol. 140, no. 12, pp. 1–12, 2014, doi: 10.1061/(asce)st.1943-541x.0001023.
13. Meisam S. G. and Cheng, J. J. R., "Steel plate shear walls with outriggers. Part II: Seismic design and performance," J. Constr. Steel Res., vol. 137, no. March, pp. 311–324, 2017, doi: 10.1016/j.jcsr.2017.04.007
14. Gholipour M., Asadi E., and Alinia M. M., "The use of outrigger system in steel plate shear wall structures," Adv. Struct. Eng., vol. 18, no. 6, pp. 853–872, 2015, doi: 10.1260/1369-4332.18.6.853.
15. Yang, Q., Lu, X., Yu, C., and Gu, D., "Experimental study and finite element analysis of energy dissipating outriggers," Adv. Struct. Eng., vol. 20, no. 8, pp. 1196–1209, 2017, doi: 10.1177/1369433216677122.
16. Pardo, K. R., Ram, K., Aye, K., Santana, C., Cornejo, K., and Chen, C., "An Analysis of Viscous Dampers in Outrigger Systems Subjected to Wind Loads and Seismic Excitations," Eng. Environ. Sci., pp. 1–33, 2019.

17. Zhou, Y., Shao, H., Cao, Y., and Lui, E. M., "Application of buckling-restrained braces to earthquake-resistant design of buildings: A review," Eng. Struct., vol. 246, no. May, 2021, doi: 10.1016/j.engstruct.2021.112991.
18. Elkahlawy, A., Shallan, O., Abd-El-Mottaleb, H., and Fathy, E., "Buckling Restrained Braces: A Review on Classifications, Design Strategy, and Applications," Egypt. Int. J. Eng. Sci. Technol., Vol. 46, issue 1, pp. 24-38, 2024, doi: 10.21608/eijest.2023.210867.1230.
19. Gupta, A and Krawinkler, H. (1999). Seismic Demands for Performance Evaluation of Steel Moment Resisting Frame Structures. John A Blume Earthquake Engineering Center Technical Report 132. Stanford Digital Repository.
20. Hemmati Khollari, M.R.; Asadi, A.; Tajammolian, H., "Seismic Fragility Assessment of SMRFs Equipped with TMD Considering Cyclic Deterioration of Members and Nonlinear Geometry," Buildings 2023, 13, 1364, doi: 10.3390/ buildings13061364.
21. Gitleman, L., and Kleberger, J., State of the Art Report on Systems Performance of Steel Moment Frames Subject to Earthquake Ground Shaking, FEMA-355C, September 2000.
22. Sabelli, R., and Bruneau, M., "Design guide 20: steel plate shear walls" American Institute of Steel Construction, Chicago, IL, USA, 2007, Accessed: Nov. 09, 2022. [Online]. Available: https://www.aisc.org/Design-Guide-20-Steel-Plate-Shear-Walls.
23. Purba, R., and Bruneau, M., "Case Study on the Impact of Horizontal Boundary Elements Design on Seismic Behavior of Steel Plate Shear Walls," Journal of Structural Engineering, vol. 138, no. 5. pp. 645–657, 2010. doi: 10.1061/(asce)st.1943-541x.0000490.
24. Purba, R., and Bruneau, M., "Seismic Performance of Steel Plate Shear Walls Considering Two Different Design Philosophies of Infill Plates. II: Assessment of Collapse Potential," J. Struct. Eng., vol. 141, no. 6, pp. 1–12, 2014, doi: 10.1061/(ASCE)st.1943-541x.0001097.
25. ASCE - American Society of Civil Engineers, "Minimum design loads and associated criteria for buildings and other structures," 2017, doi: 10.1061/9780784414248.
26. Mishra, P., and Vyavahare, A. Y., "A critical review on buckling restrained braces," Gradjevinar, vol. 75, no. 12, pp. 1165–1181, 2023, doi: 10.14256/JCE.3778.2023.
27. Puckett, J. A., Patrick McManus and Addison MacMahon, A., "Economic and serviceable seismic systems Phase II - All-bolted buckling restrained braced frames" AISC Report, University of Wyoming, February 2011.
28. CSI. SAP2000 Version 24.1.0: Integrated finite element and design of structures., "CSI. SAP2000: Integrated finite element analysis and design of structures. Computers and Structures Inc., Berkeley, California, USA. 2023."
29. Shayanfar, M., Broujerdian, V., and Ghamari, A., "Analysis of Coupled Steel Plate Shear Walls with Outrigger System for Tall Buildings," Iran. J. Sci. Technol. - Trans. Civ. Eng., vol. 44, no. 1, pp. 151–163, 2020, doi: 10.1007/s40996-019-00246-2.s